Journal of Applied Polymer Science

Preparation and properties of functionalized graphene/waterborne polyurethane composites with highly hydrophobic

Xiaomin Luo,[1,2] Peng Zhang,[1] Jing Ren,[1] Rui Liu,[1] Jianyan Feng,[2] Binghui Ge[1]

[1]College of Resources & Environment, Shaanxi University of Science & Technology, Xi'an 710021, China

[2]Xi'an Engineering Laboratory of Fiber-Based Composite Materials, Xi'an 710021, China

Correspondence to: X. Luo (E-mail: owen_pp@126.com)

ABSTRACT: The long-chain functionalized graphene nanoplatelets (FGN) were functionalized by isophorone diisocyanate and then octadecylamine, the graphene functionalized/waterborne polyurethane (WPU) composites were prepared by solution mixture. The results showed that the FGN achieved good dispersion with exfoliated and intercalated nanostructure and strong interfacial adhesion with WPU, which made the nano–composites have a significant enhancement of thermal stability and mechanical properties at low FGN loadings. With 1.5% of FGN added, the tensile strength of the composites reached the maximum of 17 MPa, which improved by 41.6%, the water absorption of the composites is only 6.7%. With the incorporation of 2 wt % FGN, and the static contact angle of the composites reached to about 120°, showing the high hydrophobicity. At the same time, the volume resistivity of the composites was changed from 2.34×10^{12} Ω·cm to 3.77×10^{9} Ω·cm. © 2015 Wiley Periodicals, Inc. J. Appl. Polym. Sci. **2015**, *132*, 42005.

KEYWORDS: functionalization of polymers; graphene and fullerenes; nanotubes; non-polymeric materials and composites; properties and characterization; resins

Received 3 November 2014; accepted 17 January 2015

DOI: 10.1002/app.42005

INTRODUCTION

The surface wettability of the material is closely related to a number of physical and chemical processes, such as adsorption, lubrication, adhesion, dispersion, and friction.[1,2] The "lotus effect" in the nature is well known, and the highly hydrophobic coating has good self-cleaning and anti-fouling ability, widely used in the textile, military, metal rust-proof, waterproof, finishing, oil, etc.[3] Especially more and more attention has been drawn on the hydrophobic conductive composite functional materials. Zhao[4] got a superhydrophobic conductive material made by multiwalled carbon nanotubes which were functionalized by methyl styrene and butyl methacrylate and he found that the material could be used in aerospace, electronics, and so on. Wu[5] prepared a super-hydrophobic multiwalled carbon nanotubes/polyvinylidene fluoride composite materials by solution blending. The study revealed that with the increase of the content of MWCNT, the hydrophobic properties of the composites were increased gradually. Recently, graphene is introduced to fabricate conductive superhydrophobic surfaces with their excellent mechanical properties, electrical properties, thermal properties, and chemical stability.[6–8] Especially, covalent grafting of polymer chains with low surface energy on the surface of graphene to fabricate conductive superhydrophobic surfaces has attracted considerable attention.[9–12]

In this article, graphene oxides were prepared by the Hummers' method.[13,14] We tried to functionalize graphene oxide with isophorone diisocyanate (IPDI), then the octadecylamine (ODA) were used to grafting modification. The graphene oxide and functionalized products were characterized by Fourier Transform Infrared Spectroscopy, X-ray diffraction (XRD), Raman spectroscopy, atomic force microscopy, and electron microscope. And the waterborne polyurethane (WPU) composites were prepared by solution mixture, and the mechanical, water resistance, heat resistance, and conductivity of composite materials were studied.

EXPERIMENTAL

Materials

Polycarbonate diol 2000 (PCDL2000), CP, Aladdin reagent (Shanghai); dibutyltin dilaurate (DBTDL), AR, Tianjin Chemical Reagent Factory; IPDI, CP, Shanghai Dibo Chemical Technology; dimethylolpropionic acid (DMPA, 98%), Aladdin Reagent (Shanghai); Dimethyl Formamide (DMF), AR, Tianjin Kemiou Chemical Reagent Development Center; n-octadecylamine (ODA), AR, Tianjin Fuyu Chemical Triethylamine (TEA, AR, Tianli Industry of Fine Chemicals, Tianjin, China) was used as the neutralization agent; 1,2-Ethanediamine (EDA, AR, Kermel Chemical Reagent, Tianjin, China) was used as a chain extender after emulsification.

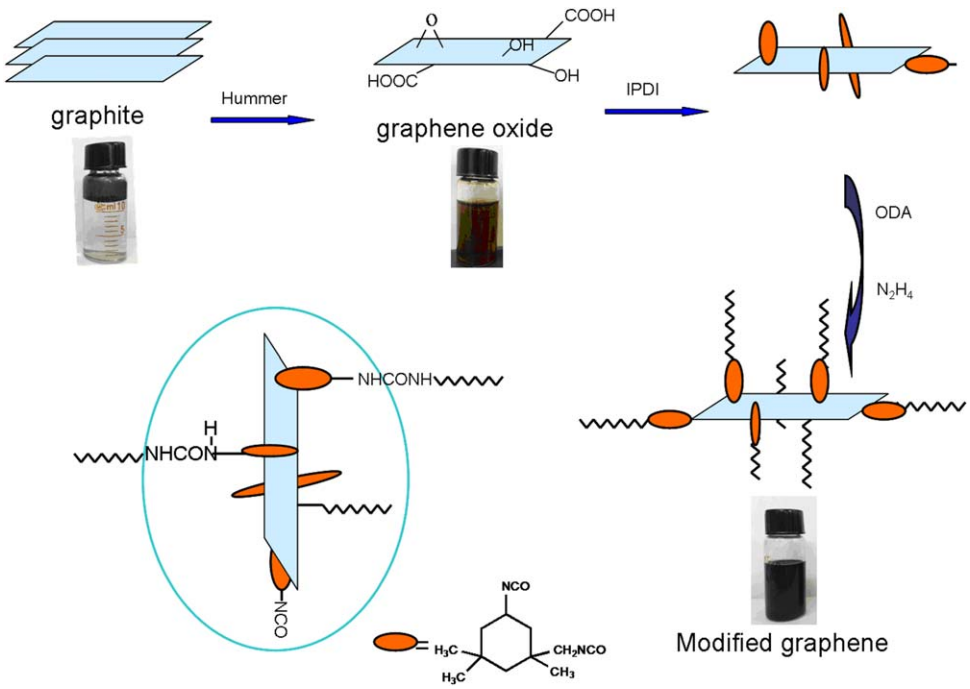

Figure 1. Preparation of a long-chain-functionalized graphene. [Color figure can be viewed in the online issue, which is available at wileyonlinelibrary.com.]

Preparation of Graphene Oxide

Graphene oxide (GO) was synthesized by Hummers' method with minor modification.[13,14] About 250 mL of H_2SO_4 was placed in a three-neck flask and cooled in an ice bath. This was followed by the addition of 3 g graphite. The mixture was stirred for 30 min at the temperatures below 5°C, after which 15 g of $KMnO_4$ was added slowly for over 60 min. After 30 min, the mixture was heated to 35°C, and the reaction was continued for 5 h. Then, the mixture was cooled and excess H_2O (120 mL) was added slowly. The unreacted $KMnO_4$ was reduced through the addition of excess aqueous H_2O_2 (30%) until bubbles were observed and the color was changed to abrilliant yellow. When the mixture was allowed to settle for 12 h, the clear supernatant was decanted, and the sediment was washed repeatedly with distilled water until the pH value of the supernatant reached to 7. The GO powder was dried in air for 1 day and then in a vacuum oven for 2 days at 65°C. To completely remove water from the GO, the powder was stored in a phosphorous pentoxide (P_2O_5)- containing desiccator for 1 week.

Preparation of the Functionalized Graphene Nanoplatelets

About 500 mg GO was dispersed into DMF (10 mg/mL) by ultrasound (400 w), then moved into the three-necked flask, 22.2 g IPDI was added, and the mixture was heated and stirred for 6 h at 80°C under nitrogen atmosphere. Then 40 g ODA was added and continued to be heated for 3 h at 70°C. Then 40 μL hydrazine hydrate was added to be heated to 100°C for 1 h. Cooled to room temperature, the products were washed by dichloromethane, ethanol, deionized water to remove the unreacted IPDI and ODA, and the products were dried to obtain a long-chain-functionalized graphene. The specific modification process was shown in Figure 1.

Preparation of WPU Emulsion

IPDI, PCDL, and DBTDL were added into a three-necked flask with a thermometer and an electric mixer at 90°C reacting for 2 h under nitrogen atmosphere. Then cooled to 70°C, DMPA was added and heated to 90°C reacting for 3 h. When cooled to room temperature, the TEA was added to be stirred for 0.5 h and the polyurethane prepolymer was obtained (acetone was added to reduce the viscosity in the reaction period). The polyurethane prepolymer was slowly added to 500 mL deionized water under high-speed stirring (2000 rpm/min). At the same time, the chain extender (EDA) was added. After stirred vigorously for 1 h, the WPU was obtained (the solid content was $35 \pm 5\%$, and the emulsion was transparent and slightly blue).

The Preparation of Functionalized Graphene/WPU Composites

The functionalized graphene nanoplatelets (FGN) was dispersed in acetone and sonicated for 30 min. The mixture of about 20 mg/mL was fed into the WPU and agitated for 1 h to get the WPU/FGN nano-composites. Finally, the lid of the reactor was opened and the emulsion was agitated for 12 h to evaporate the acetone. For measurement, the films of the nano-composite were cast on poly (propylene) plates at room temperature.

Characterization

The infrared spectroscopy was characterized by American Brooke's Verte-70 V Fourier Transform Infrared Spectrometer, the scanning range was from 4000 to 500 cm^{-1}, a resolution of 4 cm^{-1}. The XRD patterns were tested by Germany's Bruker. Test conditions were that Cu was used as Ka source, tube voltage was 40 kV, X-ray wavelength = 0.154 nm, scanning range of 2θ was 5–40°, wavelength scan was 1.54, and the scanning speed

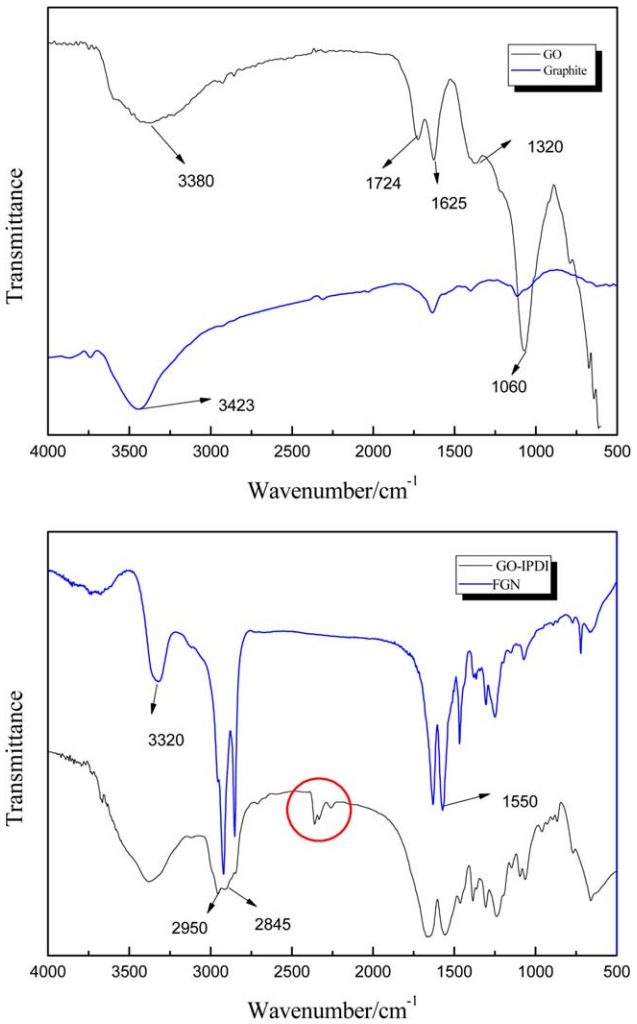

Figure 2. FTIR spectra of graphite, GO, GO-IPDI, **and** FGN. [Color figure can be viewed in the online issue, which is available at wileyonlinelibrary.com.]

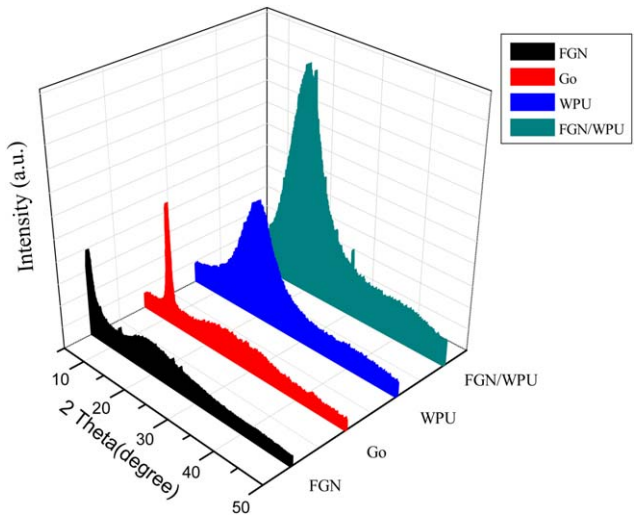

Figure 3. XRD patterns of GO, FGN, WPU and FGN/WPU. [Color figure can be viewed in the online issue, which is available at wileyonlinelibrary.com.]

was 5°/min. Raman spectroscopy (Renishaw company) analysis was done, the samples were placed on a glass slide and a 514 nm laser excitation was used in the testing process. SPA400-SP13800 Atomic Force Microscope (Digital Instruments, Seiko) was used to observe, the graphene oxide was diluted several times to form a dilute suspension and then was dropped on a smooth silicon substrate using a tapping mode to test the surface morphology and size. Wettability was characterized by an OCA20 dataphysics optical contact angle meter, German company and the contact angle was measured in five different positions to calculate the average value. TGA was characterized by the United States TA Instruments Q500. After the sample was dried *in vacuo*, test conditions were under N_2 atmosphere, the gas flow rate was 50 mL/min, heating rate was 10°C/min, and the test range was 30–600°C.

RESULTS AND DISCUSSION

Figure 2(a) showed the infrared spectra of graphite and GO. As can be seen from Figure 2, there was a significant infrared absorption peak of graphite materials at 3423 cm^{-1}. This is because of a large specific surface area of the graphite, and adsorption of water or other contaminants on its surface.[15] Compared with graphite, GO was prepared by Hummers. There were more of infrared absorption peaks, in which absorption peak was at 1724 cm^{-1} corresponding to the absorption peak of the stretching vibration of -COOH, the absorption peak was at 1625 cm^{-1} corresponding to absorption peak of the stretching vibration of C = C, the absorption peak was at 1060 cm^{-1} and the characteristic absorption peaks were from -O-. Furthermore, absorption peaks of -OH at about 3380 cm^{-1} were turned significantly wider. The presence of these oxygen-containing functional groups was described as graphene sufficiently oxidized.[16] After the graphene oxide functionalized by IPDI, the characteristic peaks appeared at 2950 and 2845 cm^{-1}, corresponding to those of the stretching vibrations of $-CH_3$ and $-CH_2$. The new peaks of GO-IPDI appeared at 2240–2270 cm^{-1}. It is the absorption peak of -NCO, which indicated that IPDI was

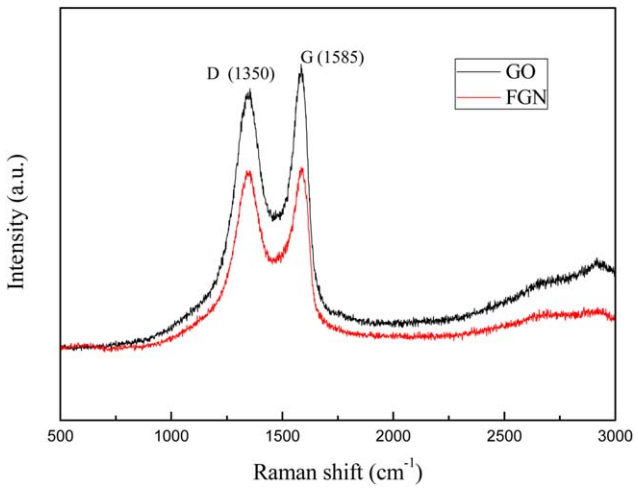

Figure 4. Raman spectra of GO and FGN. [Color figure can be viewed in the online issue, which is available at wileyonlinelibrary.com.]

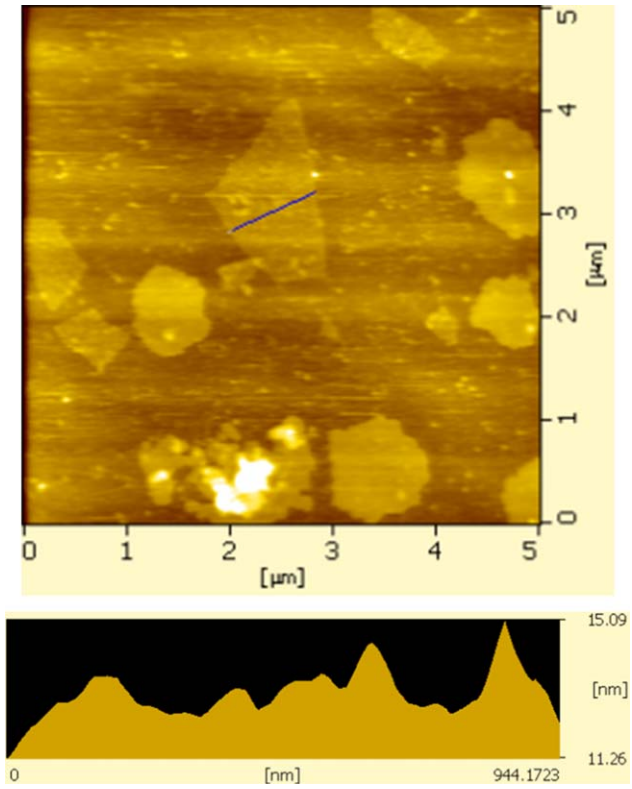

Figure 5. AFM images of GO (GO/water = 0.005 mg/L). [Color figure can be viewed in the online issue, which is available at wileyonlinelibrary.com.]

grafted or adsorbed on the graphene oxide. After the chain extension by ODA, the characteristic peaks at 2240–2270 cm^{-1} were disappeared. After deoxidation by hydrazine hydrate, the color of the long-chain functionalized graphene was changed from dark brown to black and it can be stably dispersed in the DMF in Figure1.

Figure 3 showed the XRD patterns of GO, FGN, WPU, and composite materials. The peaks of graphene oxide (GO) appeared at $2\theta = 11.3°$ corresponding to a basal spacing of d_{001}=0.786 nm. The diffraction peak of the long-chain functionalized graphene (FGN) appeared at $2\theta = 5.4°$, corresponding to the layer spacing of 1.63 nm. It showed that the layer spacing of functionalized graphene was further expanded and the stacking between layers was turned looser. The diffraction peak of WPU appeared nearby at about $2\theta = 20°$. It was because that the polyurethane itself had a plurality of repeating urethane groups and the presence of strong intermolecular forces, forming the crystals.[17] The peaks of the composites turned more significant, because the hydrogen bond was formed between the functional groups on the graphene and the matrix of the polyurethane, making the intermolecular forces strengthen.[18]

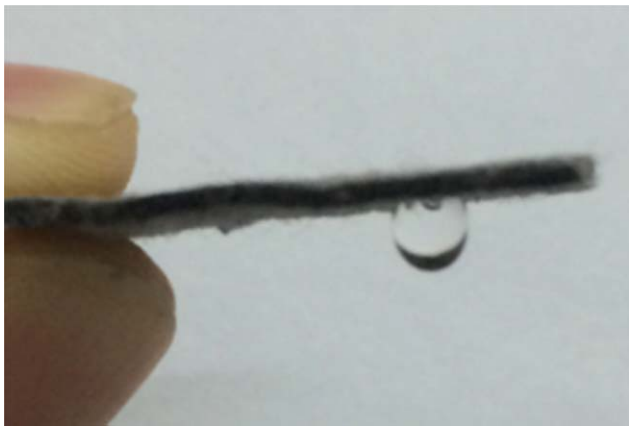

Figure 7. Water droplet was remaining in the surface when the surface is held upside down. [Color figure can be viewed in the online issue, which is available at wileyonlinelibrary.com.]

Figure 4 was the Raman spectra of GO and FGN. Graphene oxide presented in the vicinity of 1585 and 1350 cm^{-1}. It is the G-peak caused by vibration E_{2g} and D-peak caused by graphite that the conjugated structure defected.[19] The functionalized graphene in the similar position also showed peaks, but the peaks of functionalized graphene were slightly blue-shifted and the I_G/ID turned smaller. It showed that its regularity was changed, since the introduction of functional groups between the graphite layers. Atomic force microscope was used to determine the degree of exfoliation of GO in the aqueous medium and their

Figure 6. Water droplets sitting on the composite film. [Color figure can be viewed in the online issue, which is available at wileyonlinelibrary.com.]

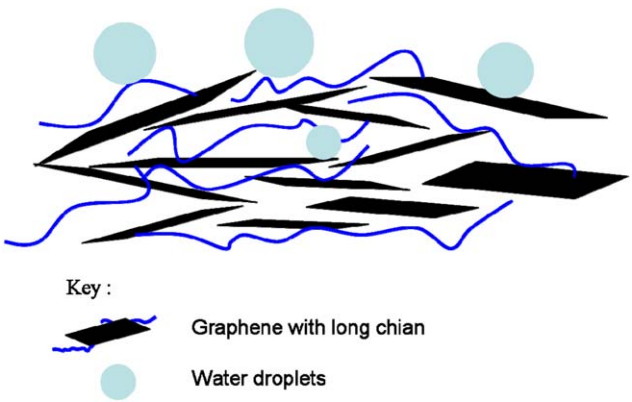

Figure 8. Schematic presentation of loading of modified graphene sheets on the film: illustrate that water droplets were obstructed into the composites by FGN with hydrophobic groups. [Color figure can be viewed in the online issue, which is available at wileyonlinelibrary.com.]

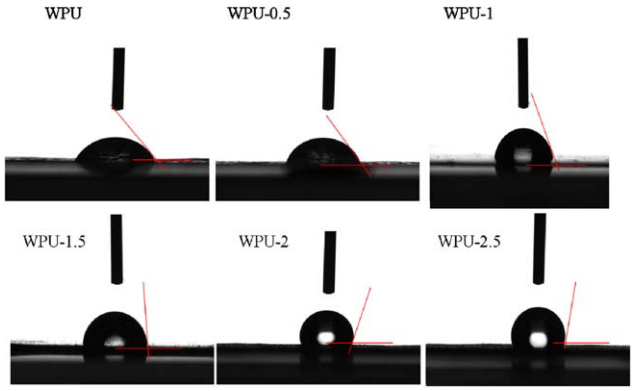

Figure 9. Static contact angles of composites. [Color figure can be viewed in the online issue, which is available at wileyonlinelibrary.com.]

lateral size and thickness. According to the AFM data obtained (Figure 5), GO in the aqueous medium (0.05 mg/mL) GO was formed with lateral size range of 1–2 μm and sheet thickness of 11–15 nm.

Figure 6 showed water droplets sitting on the composite film. As shown in Figure 7 when we expose the FGN-coated cotton textile (sample 1) to water, droplets remain on the surface when the surface was held upside down. The coating had successfully produced adhesive type hydrophobicity. The distribution of hydrophobic and hydrophilic domains on the composites because of the deposition of FGN is shown using a model in the schematic diagram of Figure 8. As the composites had more hydrophobic domains of the FGN, the water was harder to infiltrate. It is clear from the schematic diagram. Figure 9 showed the static contact angles of composites with different amounts of graphene. The static contact angle of WPU film was 65°. When the amount of graphene was 1.5%, the contact angle of the composite platform was about 90° and the hydrophilic material was changed into hydrophobic materials. When the amount of graphene reached to 2.5%, the static contact angle of the composite material reached to about 120°, showing high hydrophobicity. The surface of graphene functionalized was rich in long-chain hydrophobic functional groups, and the C=C structure of graphene also had strong hydrophobicity. In addition, the high content made the polyurethane composite material reunited more seriously, and the roughness of composites was increased on a microscopic scale, as shown in Figure 10. According to Wenzel[24] and Cassie's theory,[25] the surface roughness was one of the factors affecting the surface wettability. The hydrophobicity would be enhanced with the surface roughness increased geometrically. From Figure10 we can see that when the surface roughness of composites was Ra = 7.1, forming the structure similar to the lotus of the mastoid.

Figure 11(a,b) was the SEM image of modified graphene, showing fluffy and uniform wrinkles. To evaluate the dispersion state of fillers and interfacial bonding strength, the SEM was conducted to analyze the cryogenically fractured surface of the composites. WPU was very flat and there were no wrinkles, but the morphologies of composites were different. There were many irregular projections on the surface with some stripes in the fracture direction whereas the incorporation of FGN into the polymer resulted in the formation of many irregular

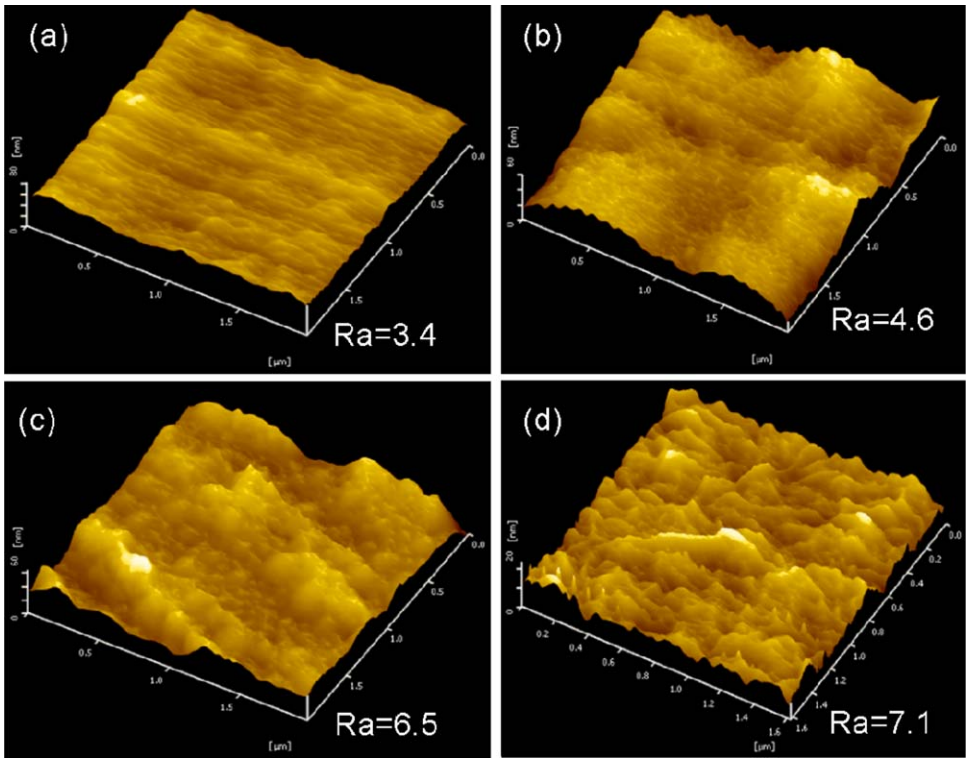

Figure 10. AFM images of the surface of (a) neat WPU, (b) WPU-0.5, (c) WPU-1, and (d) WPU-2. [Color figure can be viewed in the online issue, which is available at wileyonlinelibrary.com.]

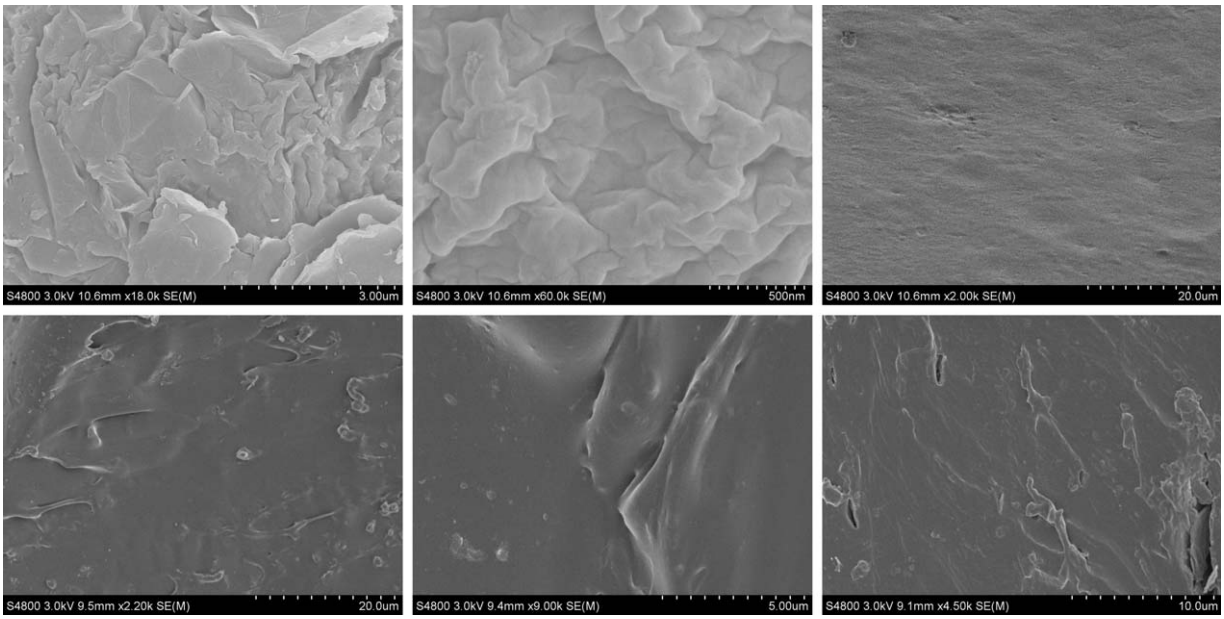

Figure 11. SEM sections images of: (a, b) FGN, (c) pure WPU, and (d, e, f) FGN/ WPU composites. [Color figure can be viewed in the online issue, which is available at wileyonlinelibrary.com.]

protuberances evenly distributed on the fracture surface, but no obvious phase separation of the interface. Graphene was wrapped in a thick polyurethane matrix together. The protrusions on the surface were because of the large specific surface area and nano-scale of the graphene.[20] It showed that the graphene with long-chain alkenyl groups had good compatibility with WPU. In general, the graphene with long chain in the WPU resin showed good adhesion and uniform dispersion. However, a partial agglomeration of graphene happened, as shown in Figure 10(f). It was because graphene functionalized had a special chemical structure on the surface and the strong force was formed with WPU.[21] Therefore, the results showed that the performance of composite materials was enhanced.

Figure 12 showed the results of the mechanical properties of the composites. It showed that the tensile strength of the polyurethane material was 12 MPa. Graphene was added to improve the tensile strength of the composite material. When the addition amount was 1.5%, the tensile strength of the composites reached to 17 MPa, which was improved by 41.6%. It was because the graphene itself had a strong strength and hardness, which was acted as a skeletal structure in the WPU matrix, improving the tensile strength of the composite material.[19,21] However, the tensile strength of the composites began to decrease, with graphene further added. It was easy to generate the particle agglomeration. When the content of graphene in the polyurethane was higher, the agglomerated particles were easily damaged to the polyurethane matrix. When the external forced the slip to be generated between the agglomeration of particles, the composite material system performance was degraded.[20,22] When the amount of graphene was less than 2%, the elongation at break of the composite material was at 600–800%.

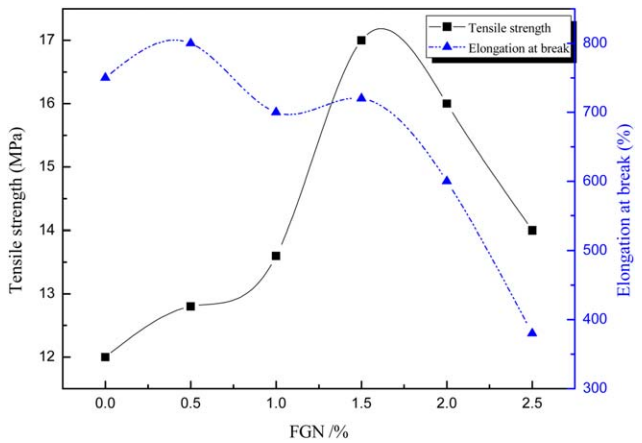

Figure 12. Mechanical properties of composites. [Color figure can be viewed in the online issue, which is available at wileyonlinelibrary.com.]

Figure 13 showed that the results of water absorption of the composites. The results showed that the water absorption of WPU was 12.5%. It was because that the molecular chain of WPU contained the hydrophilic groups, showing the strong water absorption. With the addition of FGN, the water absorption of composites was reduced. With the addition of GO, the water absorption of composites was also a little reduced. When the addition amount was of 1.5% FGN, the water absorption of the composite material was 6.7%. The surface of the functionalized graphene contained a large amount of hydrophobic groups. And reduced by hydrazine hydrate, oxygen functional groups of graphene were partially removed, showing the higher hydrophobicity. Layered graphene sheets were piled into a shielding layer of water molecules, effectively reducing the rate of penetration of water molecules.[23]

Table I was the volume resistivity data of composites with different amounts of FGN added. As can be seen from table, the volume resistivity of the neat WPU was 2.34×10^{12} Ω cm, belonging

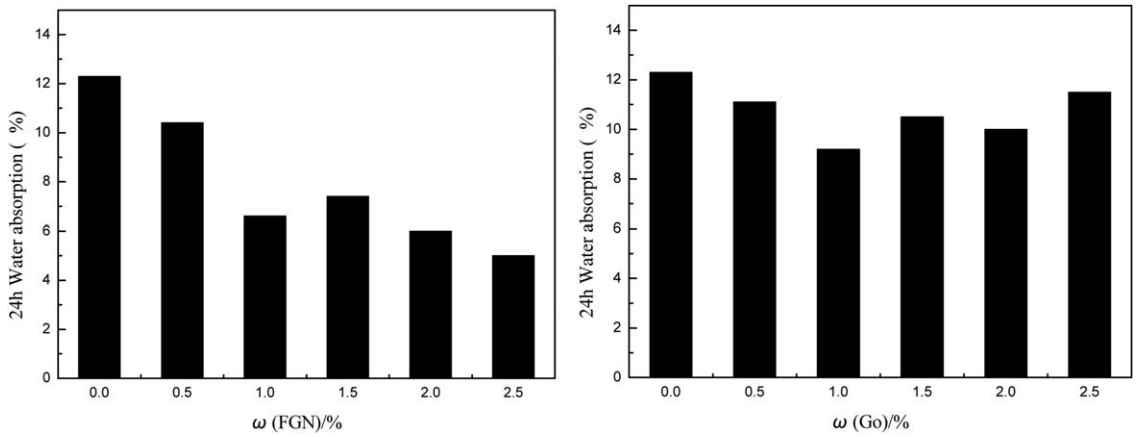

Figure 13. Water absorption of the composite materials.

Table I. Volume Resistivity of Neat WPU and Composites

	WPU	WPU-0.5	WPU-1	WPU-2	WPU-2.5
Film thickness (mm)	0.23	0.18	0.15	0.24	0.18
Volume resistivity (Ω·cm)	2.34×10^{12}	1.07×10^{12}	9.98×10^{11}	3.77×10^{9}	5.46×10^{8}

to insulating material. With the graphene added, the volume resistivity of the composite was decreased. When the amount of graphene was exceeded by 2%, the resistance of the composite material showed a sudden decreasing change, which indicated that graphene in the polyurethane matrix was overlapped each other, forming a relatively complete conductive network.

Figure 14 showed the TGA results of graphene/WPU composites. As can be seen, the thermal decomposition of the composites had two phases: the range of the first stage of decomposition was at 230–350°C, which was corresponded to the thermal decomposition of the hard segment of polyurethane. The range of the second stage of decomposition was at 380–410°C, which was corresponded to the thermal decomposition of the soft segment of polyurethane.[26] With the addition of FGN, the thermal decomposition rate of the composites was slow. It was because the graphene had high surface area, so as to form a barrier effect in the polyurethane system.[27]

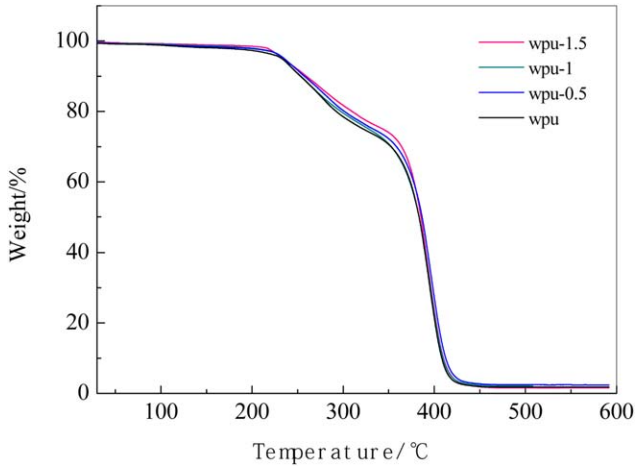

Figure 14. TGA of WPU, WPU-0.5, WPU-1, and WPU-1.5. [Color figure can be viewed in the online issue, which is available at wileyonlinelibrary.com.]

CONCLUSIONS

In this study, a simple way is proposed to prepare the long-chains graphene with good dispersibility. The results of AFM and SEM show that the functionalized graphene can possess good compatibility with WPU, the good adhesion is formed and the mechanical property of composites is improved. Meanwhile, the functionalized graphene can make polyurethane high hydrophobicity. The TGA results show that the heat shield is formed by graphene in the polyurethane matrix. Therefore, the thermal stability of the composite material is enhanced. Graphene prepared by this method shows great potential in improving the physical properties of the polymer.

ACKNOWLEDGMENTS

The authors are grateful to the Science and Technology Bureau Program Foundation of Xi'an (CXY1344); Shaanxi University of Science and Technology Innovation Team (TD12-04).

REFERENCES

1. Sethi, S.; Dhinojwala, A. *Langmuir* **2009**, *25*: 4311.
2. Wang, L.; Yang, S.; Wang, J.; Wang, C.; Chen, L. *Mater. Lett.* **2011**, *65*, 869.
3. Feng, X. J.; Jiang, L. *Adv. Mater.* **2006**, *18*, 3063.
4. Zhao, L.; Liu, W. L.; Zhang, L. D.; Yao, J. S.; Xu, W. H.; Wang, X. Q.; Wu, Y. Z. *Colloids Surf. A Physicochem. Eng. Asp.* **2013**, *423*, 69.

5. Wu, T.; Pan, Y.; Li, L. *Colloids Surf. A Physicochem. Eng. Asp.* **2011**, *384*, 47.
6. Choi, B. G.; Park, H. S. **The** *J. Phys. Chem. C* **2012**, *116*, 3207.
7. Singh, E.; Chen, Z .; Houshmand, F.; Ren, W.; Peles, Y.; Cheng, H. M.; Koratkar, N. *Small* **2013**, *9*, 75.
8. Zha, D.; Mei, S.; Wang, Z.; Li, H.; Shi, Z. J.; Jin, Z. X. *Carbon* **2011**, *49*, 5166.
9. Zhou, Y.; Xu, F.; Jiang, G.; Wang, X. H.; Hu, R. B.; Wang, R. J.; Xi, X. G.; Wang, S. *Powder Technol.* **2012**, *230*, 247.
10. Zheng, F.; Deng, H.; Zhao, X.; Li, X.; Yang, C.; Yang, Y. Y.; Zhang, A. *J. Colloid Interface Sci.* **2014**, *421*, 49.
11. Li, J.; Ling, J.; Yan, L.; Wang, Q.; Zha, F.; Lei, Z. *Surf. Coat. Technol.* **2014**.
12. Hong, J.; Kang, S. W. *Colloids Surf. A Physicochem. Eng. Asp.* **2011**, *374*, 54.
13. Geng, Y.; Wang, S. J.; Kim, J. K. *J. Colloid Interface Sci.* **2009**, *336*, 592.
14. Zheng, Q. B.; Ip, W. H.; Lin, X. Y.; Yousefi, N.; Yeung, K. K.; Kim, J. K. *ACS Nano* **2011**, *5*,6039.
15. Song, P.; Cao, Z. H.; Cai, Y. Z.; Zhao, L. P.; Fang, Z. P.; Fu, S. Y. *Polymer* **2011**, *52*, 4001.
16. Li, J.; Kim, J. K.; Sham, M. L.; Marom, G. *Compos. Sci. Technol.* **2007**, *67*, 296.
17. Cai, D.; Yusoh, K.; Song, M. *Nanotechnology* **2009**, *20*, 085712.
18. Kim, H.; Macosko, C. W. *Macromolecules* **2008**, *41*, 3317.
19. Choi, S. H.; Kim, D. H.; Raghu, A. V.; Reddy, K. R.; Lee, H.; Yoon, K. *J. Macromol. Sci. B* **2012**, *51*, 197.
20. Sugihara, S.; Sugihara, K.; Armes, S. P.; Ahmad, H.; Lewis, A. L. *Macromolecules* **2010**, *43*, 6321.
21. Wu, C.; Huang, X.; Wang, G.; Wu, X.; Yang, K.; Li, S.; Jiang, P. *J. Mater. Chem.* **2012**, *22*, 7010.
22. Qi, X.; Tan, C.; Wei, J.; Zhang, H. *Nanoscale* **2013**, *5*, 1440.
23. Liao, K. H.; Park, Y. T.; Abdala, A.; Macosko, C. *Polymer* **2013**, *54*, 4555.
24. Nakae, H.; Inui, R.; Hirata, Y.; Saito, H. *Acta Mater.* **1998**, *46*, 2313.
25. Cassie, A. B. D. *Discuss. Faraday Soc.* **1948**, *3*, 11.
26. Cai, D.; Jin, J.; Yusoh, K.; Rafiq, R.; Song, M. *Compos. Sci. Technol.* **2012**, *72*, 702.
27. Kim, H.; Miura, Y.; Macosko, C. W. *Chem. Mater.* **2010**, *22*, 3441.